SCIPEDIA Revista Internacional de Métodos Numéricos para Cálculo y Diseño en Ingeniería

Revista Internacional Métodos numéricos para cálculo y diseño en ingeniería RIMNI

Efficiency Maximization of a Jet Pump for an Hydraulic Artificial Lift System

Rogelio de Jesús Portillo-Vélez[1], J. A. Vásquez-Santacruz[1], L. F. Marín-Urías[1], Adelfo Vargas[1], P. García-Ramírez[1], J. L. Morales-de-la-Mora[2], A. L. Vite-Morales[2], E. A. Gutierrez-Domínguez[3]

1 Universidad Veracruzana

2 Geolis/Nuvoil

3 Instituto Nacional de Astro-física, Óptica y Electrónica

Abstract

This work presents a simpler numerical design method for efficiency maximization of an Hydraulic Jet Pump (HJP) for oil-well extraction process, considering its hydraulic and geometric parameters. The design process consists in setting and solving a constrained non-linear optimization problem by taking into account the hydraulic model of the HJP in terms four design variables: throat area, nozzle area, injection flow, and injection pressure to the oil-well. The objective function of this case aims to maximize the HJP's efficiency avoiding to approach cavitation condition as well fulfilling technical constraints. A numerical technique, Differential Evolution Algorithm (DEA), has been implemented to solve the optimization problem. The proposed methodology leads to a solution set by considering only commercial geometries and feasible operating conditions for the HJP, which facilitates its practical implementation. A set of ten oil-wells with land production data, operating in the southeaster of Mexico, is used to compare and validate several Jet pump designs, i. e., through comparison with actual oil-well's operation condition.

OPEN ACCESS

Published: 08/02/2019

Accepted: 21/09/2018

Submitted: 14/06/2018

DOI: 10.23967/j.rimni.2018.11.002

Keywords:
optimization
efficiency
jet pump
differential evolution

1. Nomenclature

This section describes all the nomenclature used in this work.

A_n= Flow area of nozzle, [in^2].

A_s= Suction area, [in^2].

A_{th}= Flow area of throat, [in^2].

$b = A_n/A_{th}$ Nozzle to throat area ratio, [-]

G_w= Fluid column gradient, [Psi/ft].

h_1= Pump setting depth, [ft].

H=Dimensionless head recovery ratio, [-].

H_v= Jet velocity, [-].

K_j= Nozzle loss coefficient,[-].

K_d= Diffuser loss coefficient, [-].

K_s= Suction loss coefficient, [-].

K_t= Throat loss coefficient, [-].

M= Dimensionless flow ratio, [-].

M_c=Cavitation limited flow ratio, [-].

N= Index of Losses by Friction, [-].

P_1= Pressure at the entrance of the nozzle, [Psi].

P_2=Pressure at the output of the throat, [Psi].

P_3= Pressure at the intake of the HJP, [Psi].

P_s= Injection pressure (Surface pressure), [Psi].

P_f= Average oil-well pressure, [Psi].

PI= Productivity index [-].

P_v=Vapor pressure, [Psi].

P_{wf}= Flowing bottom hole pressure, [Psi].

q_1=Injection flow, [Barrels/Day (BPD)].

q_3=Production flow, [BPD].

q_2=Sum of injection and production flows, [BPD].

q_{max}= Maximum oil flow from the oil-well, [BPD].

σ= Cavitation index [-].

η= HJP efficiency [-].

γ = Specific gravity [-].

Correspondence: Rogelio de Jesús Portillo-Vélez (rogelio.portillo.velez@gmail.com, rportillo@uv.mx), J. A. Vásquez-Santacruz (alejanvasquez@uv.mx), L. F. Marín-Urías (luismarin@uv.mx), Adelfo Vargas (adelfovm@gmail.com), P. García-Ramírez (jagarcia@uv.mx), J. L. Morales-de-la-Mora (jorge.morales@geolis.mx), A. L. Vite-Morales (ana.vite@geolis.mx), E. A. Gutierrez-Domínguez (edmundo@inaoep.mx).

HP = HJP Horsepower [hp].

F = Mutation factor [-].

CR = Crossover factor [-].

2. Introduction

The challenge of finding new technologies for production and/or improving existing ones in the oil and gas industry, is shaped because of the continuous increase in demand for and rapid depletion of this non-renewable natural resource. Oil has been found naturally in large sedimentary basins at different depths ranging from 15 to 8,000 meters, occupying the empty space of porous and permeable rocks known as oil-well. As time goes by, the natural pressure of an oil-well decreases, until it can not longer produce naturally. This problem gives rise to use Artificial Lift Systems (ALS), as a feasible engineered system to exploit the oil-wells. Indeed, is the fact that more than 95% of the world's oil-wells use some ALS, starting from the oldest and simplest one such as mechanical pumping and pneumatic pumping, to the most technologies such as Electrical Submersible Pumping and hydraulic pumping.

In this work, we focus on the ALS of Hydraulic pumping with an HJP, [1]. Hence, HJPs are of vast interest in petroleum engineering because of their design characteristics, and volumetric oil production they can handle. For the Hydraulic ALS, the HJP is introduced into the oil-well via the production pipe and it can be retrieved by simply reversing the working flow sense. In this application, the HJP has some disadvantages such as the cavitation phenomenon and typically low efficiency; nevertheless, both might be mitigated by an optimum design of the HJP and the selection of the best operating conditions for the ALS.

In general, the fundamental parts of this ALS are: a combustion engine that drives a hydraulic piston (or geared) pump; an horizontal three-phase separator containing the mixture (oil, gas and sand) extracted from the oil-well; a control panel that controls the ALS and finally the HJP, installed at the bottom of the oil-well. Note that an HJP includes in a carrier that encloses the nozzle and throat (Figure 1).

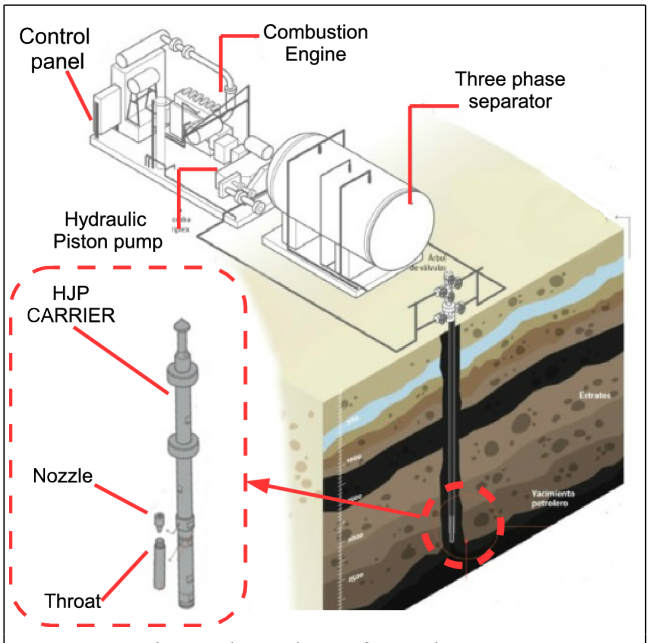

Figure 1: Schematic diagram of an ALS whit an HJP

Early works on HJP design have considered either experimental or numerical approaches or a mix of both. Mallela [2], computed normalized geometries which leads to maximum efficiencies without considering the cavitation phenomenon. S. Mohan [3], reported a numerical analysis and an optimization of an HJP via multi-surrogate model without considering cavitation. In Mohan's study, the area ratio, mixing-tube length to diameter ratio and setback ratio, were varied during an optimization process. In the work of Saker [4], it was pointed out the importance and influence of factors such as cavitation phenomena, which impact the HJP performance. In a more recent paper [5], Xiao presented a numerical and experimental study on the HJP performance and inner flow details of annular Jet pumps under three area ratios. Xiao's results included cavitation phenomenon and indicate that by decreasing outlet pressure, the cavitation generated at the throat inlet renders unstable effects for the HJP. In 2013 [6], the Norwegian University of Science and Technology (NTNU) analyzed oil-wells from the North Sea, by using the principles of the HJP, as those described in [1], to search for an optimal operational conditions of the HJP , i.e. pressures and flows. In a study closer to our approach for the HJP design, J. Fan. [7] developed a design oriented to improve the HJP efficiency by using an analytical approach that considers a computational fluid dynamics (CFD) model. Then, the influence of the pump's geometry on its performance and the CFD simulation results were used to build surrogate models of the pump's behavior. Finally, a global optimization was carried out by means of a genetic algorithm. Works surveyed so far require either extensive experimental data or CFD simulations to provide HJP performance improvement; this can be too costly and time consuming for the oil-well industry needs. For this reason, the creation of a numerical tool to determine the optimal geometric design and operational hydraulic conditions of an HJP is of paramount importance to satisfy industry requirements.

This work introduces a numerical design methodology to maximize the efficiency of an HJP, based on its hydraulic and geometrical models. According to this, the method is based on geometric and hydraulic models transcription into a constrained non-linear optimization problem with four design variables: throat and nozzle areas, the input working fluid flow and the input pressure. The objective function of the optimization problem aims to render the maximum efficiency without reaching the cavitation condition for the HJP and fulfilling technical constraints. Because of the non-linear characteristics and the number of the independent variables, a Differential Evolution Algorithm (DEA) is implemented to solve the optimization problem. As a strategy to calibrate the algorithm, only commercial geometries and real operating conditions for the HJP were used. Evidence on the feasibility of using this algorithm in real applications is demonstrated by comparisons of numerical results with ongoing oil-well production by using HJPs in the southeaster by the Mexican Company, Geolis/Nuvoil. It is important to highlight that feasible HJP geometries and operational conditions are be obtained without extensive simulations or experimentation.

This paper is structured as follows. Section 3 concerns the mathematical models considered, then the problem statement for this work is stated in Section 4. Section 5 of this paper, explains the solution methodology by using the DEA. In Section 6, numerical results are shown and analyzed, and finally Section 7 closes the paper with the conclusions and future work.

3. Mathematical models

The fundamental of operation of an HJP of an ALS is based on the Venturi principle [8]. Basically, this principle consists of applying additional energy to the oil at the bottom of the oil-

well, in order to force the fluid to flow to the surface. For this purpose, a driving or working fluid (typically water) is injected through the production pipe to the oil-well. At the return, the mixture between working fluid and oil, is forced to circulate through the annular space between the production and cladding pipes; this working principle is shown in Figure 2.

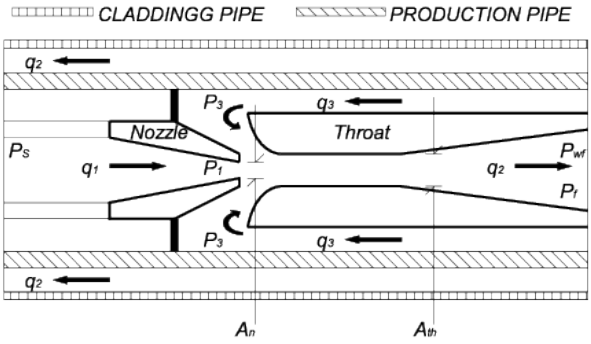

Figure 2: HJP schematic set-up

In order to improve the performance of a HJP, selection of the computational method gives rise to two options. One approach considers the use of pressures and flow ratios [9]. Although it is one of the most used, it is not adequate because in some cases relevant information is insufficient. In a second approach, experimental information such as adimensional coefficients, is used to perform the computations of the HJP efficiency [1].

In this work, we consider the hydraulic model of the HJP described in [1]. The efficiency of a HJP is defined as the ratio of the energy added to the production fluid in relation to the energy lost by the injection fluid. Therefore, we can compute the hydraulic efficiency of the pump as in equation (1), where M is the input to net production flow ratio as expressed in equation (2), and H represents the dimensionless head recovery ratio, as in equation (3).

$$\eta = M \cdot H \tag{1}$$

$$M = \frac{q_3}{q_1} \tag{2}$$

$$H = \frac{P_2 - P_3}{P_1 - P_2} = \frac{1 - N}{N + M} \tag{3}$$

In equation (2), q_3 represents the flow from the well in barrels per day (BPD) and q_1 represents the flow injected from the surface in BPD. A third flow q_2 is the sum of both flows, as shown in Figure 2. Note that the input flow q_1 can be controlled via a hydraulic (piston or geared) pump on the surface.

With respect to Equation (3), it presents has a dual definition. On the one hand, in this equation, H represents the dimensionless head recovery ratio for the pressures P_1, P_2 and P_3 of the HJP. On the other hand, the term N represents experimental information considering friction loss coefficients K_j, K_s, K_t, K_d and the geometry of the HJP, [1]. Given the values of M, the adimensional coefficients, and once the nozzle area A_n and throat area A_{th} are selected to compute b, then N is obtained using equation (4), see [1].

$$N = \frac{\left[(1+K_j) + (1+K_s)M^3\left(\frac{b}{1-b}\right)^2 + (1+K_t+K_d)(1+M)^3b^2 - 2b\right.}{\left[(1+K_j) - (1+K_s)M^2\left(\frac{b}{1-b}\right)^2\right.} \quad \left.M) - 2\frac{b^2}{(1-b} \right. \tag{4}$$

Pressure P_1, can be expressed by equation (5), as the sum of the pressure generated by the column of fluid at the production pipe and the surface pressure P_s given by an hydraulic pump.

$$P_1 = h_1 G_w + P_s \tag{5}$$

Because of the damage problems associated with cavitation phenomenon (to be considered in the following section), it is also desirable to compute the intake pressure P_3 while the pump is operating. This can be accomplished from the input flow q_1 at the nozzle, according to equation (6). Note that the intake pressure depends on the input flow, the surface pressure, and the selection of the nozzle area. It is important to remark that, once M and N are computed, pressure P_2 is obtained from equation (3).

$$P_3 = P_1 - \gamma\left(\frac{q_1}{1215.5A_n}\right)^2 \tag{6}$$

The flow from the oil-well q_3 is one of the most challenging data to obtain. When the performance of oil-well is considered, it is often assumed that it can be estimated by the productivity index [9]. This concept is only applicable for oil-wells producing under single-phase flow conditions, i.e. pressures above the oil-well fluid's bubble-point pressure. For oil-well pressures less than the bubble-point pressure, the oil-well fluid presents a two-phase behavior, gas and liquid; then, other techniques must be applied to predict oil-well performance. In this work, we consider the case when the fluid exists as two phases, oil and gas. Thus, to estimate the production rate q_3, a Vogel's performance relationship is considered [10]. In Vogel's relationship, to estimate the maximum oil production rate q_{max} from the oil-well, it is required to measure the real oil production rate q_3 and flowing bottom-hole pressure P_{wf} from a production test. Then, to obtain an measure (or estimate) of the average oil-well pressure P_f at the time of the test, equation (7) is used.

$$q_{max} = \frac{q_3}{\left[1 - 0.2\left(\frac{P_{wf}}{P_f}\right) - 0.8\left(\frac{P_{wf}}{P_f}\right)^2\right]} \tag{7}$$

The maximum oil production rate q_{max} can be used to estimate the production rates q_3 for other flowing bottom hole pressures P_wf^* at the current average oil-well pressure P_f as in equation (8). Moreover, in the following we set $P_wf^* = P_3$.

$$q_3 = q_{max}\left[1 - 0.2\left(\frac{P^*_{wf}}{P_f}\right) - 0.8\left(\frac{P^*_{wf}}{P_f}\right)^2\right] \tag{8}$$

4. Problem Statement

By considering the hydraulic models presented in the last section, the efficiency of the pump depends mainly on four operational variables: the nozzle area A_n, throat area A_{th}, the input working flow ratio q_1 and the surface pressure P_s. System pressures are computed with equations (5) - (6), loss coefficients in equation (4) also affect the HJP efficiency, nevertheless they are considered as constants taken from the literature [1] (Table 3).

The objective function of the optimization problem, represents a mathematical model that allows to quantify the performance of the HJP. In this case, we consider to maximize the HJP efficiency, defined in equation (1). Although hydraulic pumping is an effective and reliable system, it presents some operational risks and disadvantages that are considered by means of the following constraints.

The first constraint is related to the cavitation problem in the HJP [5]. The high speed that is generated between the nozzle and throat, combined with the presence of gas and other solid particles causes cavitation, i.e. the sudden formation of small vapor bubbles into the liquid oil. This is a fundamental phenomenon to be considered because it might cause considerable efficiency decrease and severe damage to the nozzle and throat of the HJP. The mathematical expression of the cavitation is represented by the limit flow ratio M_c [11], as in equation (9)

$$M_c = \frac{1-b}{b}\sqrt{\frac{P_3 - P_v}{\sigma H_v}} \tag{9}$$

To compute the Jet velocity H_v, equation (10) is used.

$$H_v = \frac{P_1 - P_3}{(1+K_j) - (1+K_s)M^2(\frac{1-b}{b})^2} \tag{10}$$

Substituting (10) into equation (9), then equation (11) is obtained, where P_v has been set to zero because low gas-oil ratio (GOR) relationships for the studied oil-wells are assumed. In the case that M is less than M_c, there is a low risk of cavitation in the HJP and efficiency might be increased.

$$M_c = \frac{1-b}{b}\sqrt{1+K_j}\sqrt{\frac{P_3}{\sigma(P_1 - P_3) + P_3}} \tag{11}$$

A second set of constraints arise from geometrical characteristics of the HJP performance, specifically related to the commercial availability of nozzle and throat produced by manufacturers. Some technical guidelines are considered as follows. Both, nozzle and throat, use a strict progression of diameter and holes provided by the manufacturer, as depicted in Table 1. The progression establishes areas of ratio between nozzles and throats. In general, high flow volumes renders low lifting and vice versa. Very small area ratios are used in shallow wells, also the injection pressure is very low for these cases. The largest area ratios are installed for high lifting heads, but this is only applicable in specific cases, [12].

The working fluid (water) and the production fluid (oil and gas), must go through the throat area A_{th}. The suction area (A_s) is the separation between the nozzle and throat; this area is where the oil-well fluid enters and it also raises a constraint. Moreover, the relationship b is also constrained by maximum and minimum values due to practical implementations. Considering this, the geometric constrains described above can be mathematically stated as follows:

- The nozzle area A_n must be smaller than the throat area A_{th}. This fact implies the existence of the suction area $A_s = A_{th} - A_n$.
- To allow enough fluid production flow, the annular suction area A_s, must be bounded as follows: $A_{s_{min}} < A_s < A_{s_{max}}$.
- Commercial nozzle and throat are considered to identify their components by the nozzle to throat ratio b; therefore: $b_{min} < b < b_{max}$.

In addition, equation (3) and Vogel relationship given by equation (8), renders a set of constraints for the systems pressures in order to get feasible (positive) values for H and q_3, this is:

- System pressures must be computed to satisfy: $P_3 < P_2 < P_1$.
- Inlet pressure must satisfy: $0 < P_3 < P_f$

After the above considerations, we propose to set the design of a HJP as solving the following constrained non-linear optimization problem:

$$\max \eta = M \cdot H$$

subject to the hydraulic pump model functions (2) - (8), the cavitation constraints (9) - (11) and the following geometrical and hydraulic constraints:

$$\begin{gathered} M < M_c \\ A_n < A_{th} \\ A_{s_{min}} < A_s \\ A_s < A_{s_{max}} \\ b_{min} < b \\ b < b_{max} \\ P_2 < P_1 \\ P_3 < P_2 \\ P_3 < P_f \\ 0 < P_3 \end{gathered}$$

The solution to this problem offers an optimum configuration of the variables A_n, A_{th}, q_1 and P_s; so that the efficiency is maximized without cavitation problems and considering implementable nozzle and throat areas. This is, it will be possible to extract as much fluid as possible with the least amount of energy possible, thus saving on the pumping equipment to be used.

5. Optimization design process using Differential Evolution

There exist several theoretical and numerical techniques, to solve non-linear constrained optimization problems. In this work, we consider a numerical approach by using a Differential Evolution Algorithm (DEA), [13]. A DEA is a numerical method for the determination of the global minimum or maximum, for highly non-linear problems. It can handle an optimization problem with or without constraints, based on a process of natural selection that imitates biological evolution, [14]. The DEA repeatedly updates a set of P initial vector designs $[\mathbf{x}_{1,0}, \mathbf{x}_{2,0}, \ldots, \mathbf{x}_{P,0}]$ called *population*, in order to reach a final set of vector designs $[\mathbf{x}_{1,f}, \mathbf{x}_{2,f}, \ldots, \mathbf{x}_{P,f}]$, for which an objective function $f(\mathbf{x}_{i,f})$ is minimized or maximized for $i = 1, 2, \ldots, P$, as shown in Figure 3.

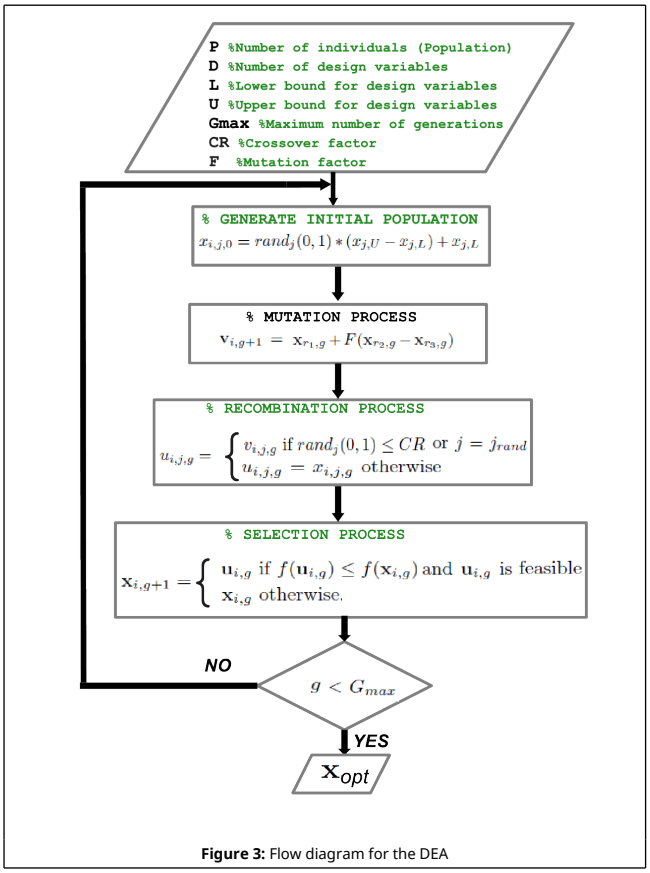

Figure 3: Flow diagram for the DEA

The design vector is defined as $\mathbf{x} = [x_1, x_2, \ldots, x_D]^T$, where D is the number of design variables; and the objective function is $f(\mathbf{x})$. It is important to mention that the design vector might belong to a set $\Omega = \{\mathbf{x}: \mathbf{x}_{min} \le \mathbf{x} \le \mathbf{x}_{max}\}$. In the following, we assume the search for a minimum of the objective function f, while for searching maximum $-f$ must be considered. Each population, is a set of vector designs $\mathbf{x}_{i,g}$, where sub-index i represents the $i-th$ vector design for the $g-th$ generation for $i = 1, 2, \ldots, P$.

The initial population for $g = 0$, can be randomly obtained for the j_{th}-component of the vector $\mathbf{x}_{i,0}$ as: $x_{i,j,0} = rand_j(0, 1) * (x_{j,U} - x_{j,L}) + x_{j,L}$ where $x_{j,L}$ and $x_{j,U}$ represents, respectively, lower and upper bounds for each variable of the vector design and $rand_j(0,1)$ is a random number between 1 and 0.

At each generation g, the DEA algorithm randomly selects individual solutions from the current population and uses them as parents to produce the offspring of the next generation. This is known as *mutation* and it states that the vector design for the next generation can be computed as $\mathbf{v}_{i,g+1} = \mathbf{x}_{r_1,g} + F(\mathbf{x}_{r_2,g} - \mathbf{x}_{r_3,g})$, where r_1, r_2 and r_3 are integers randomly selected from the set $\{1, 2, 3, \ldots P\}$, and F is a *mutation* factor. To guarantee that $v_{i,g+1} \in \Omega$ if $v_{i,j,g+1} \le x_{j,min}$ then $v_{i,j,g+1} = 2x_{j,min} - v_{i,j,g+1}$ else if $v_{i,j,g+1} \ge x_{j,max}$ then $v_{i,j,g+1} = 2x_{j,max} - v_{i,j,g+1}$.

To complement the mutation strategy, in DEA it is defined a *recombination* process that ensures each design vector copied from two different vectors, crosses with a mutant vector. This is, DEA generates a trial crossed vector $\mathbf{u}_{i,g}$ with the following definitions for its $j-th$ component: $u_{i,j,g} = v_{i,j,g}$ if $rand_j(0, 1) \le CR$ or $j = j_{rand}$ or $u_{i,j,g} = x_{i,j,g}$ otherwise, where CR is a user-defined crossover value that controls the fraction of parameter values that are copied from the mutant and j_{rand} is a randomly chosen index from the set $\{1, 2, \ldots, D\}$.

Finally, the selection is performed by comparing each trial vector $\mathbf{u}_{i,g}$ with the target vector $\mathbf{x}_{i,g}$ as follows: $\mathbf{x}_{i,g+1} = \mathbf{u}_{i,g}$ if $f(\mathbf{u}_{i,g}) \le f(\mathbf{x}_{i,g})$ and $\mathbf{u}_{i,g}$ is feasible, or $\mathbf{x}_{i,g+1} = \mathbf{x}_{i,g}$ otherwise. The algorithm continues checking feasible individuals using the constraint handling mechanism proposed in [15], for each vector of the $g-th$ generation, until some criterion is fulfilled, e.g. a maximum number of generations G_{max} is overcome or other.

After G_{max} successive generations, the population *evolves* towards a set of optimal solutions $\mathbf{x}_{i,G_{max}} = \mathbf{x}_{i,opt}$ for $i = 1, 2..., N_P$, which in this case render feasible and optimal designs of the HJP and its operational conditions.

5.1 Remarks on the algorithm implementation

Continuing with the solution to the optimization problem, it is necessary to establish the dimensions that will have nozzle and throat according to standard sizes and relationships offered by manufacturers. Figure 4 depicts in red squares commercial nozzle and throat.

Figure 4: Throat and nozzle for an HJP.

There are many manufacturers of HJPs in the world. In Table 1, the nozzle and throat areas (in squared inches) are classified for three different manufacturers: Kobe, National and Guiberson. In this paper we select the last one, since Geolis/Nuvoil company uses Guiberson Jet pumps.

Table 1. Designation of commercial nozzle and throat areas.

KOBE				NATIONAL				GUIBERSON			
Nozzle		Throat		Nozzle		Throat		Nozzle		Throat	
1	0.0024	1	0.0060	1	0.0024	1	0.0064	DD	0.0016	000	0.0044
2	0.0031	2	0.0077	2	0.0031	2	0.0081	CC	0.0028	00	0.0071
3	0.0040	3	0.0100	3	0.0039	3	0.0104	BB	0.0038	0	0.0104
4	0.0052	4	0.0129	4	0.0050	4	0.0131	A	0.0055	1	0.0143
5	0.0067	5	0.0167	5	0.0064	5	0.0167	A+	0.0075	2	0.0189
6	0.0086	6	0.0215	6	0.0081	6	0.0212	B	0.0095	3	0.0241
7	0.0111	7	0.0278	7	0.0103	7	0.0271	B+	0.0109	4	0.0314
8	0.0144	8	0.0359	8	0.0131	8	0.0346	C	0.0123	5	0.038
9	0.0186	9	0.0464	9	0.0167	9	0.0441	C+	0.0149	6	0.0452
10	0.0240	10	0.0599	10	0.0212	10	0.0562	D	0.0177	7	0.0531
11	0.0310	11	0.0774	11	0.0271	11	0.0715	E	0.0241	8	0.0661
12	0.0400	12	0.1000	12	0.0346	12	0.0910	F	0.0314	9	0.0804
13	0.0517	13	0.1292	13	0.0441	13	0.1159	G	0.0452	10	0.0962
14	0.0668	14	0.1668	14	0.0562	14	0.1476	H	0.0661	11	0.1195

15	0.0863	15	0.2154	15	0.0715	15	0.1879	I	0.0855	12	0.1452
16	0.1114	16	0.2783	16	0.0910	16	0.2392	J	0.1257	13	0.1772
17	0.1439	17	0.6594	17	0.1159	17	0.3146	K	0.1590	14	0.2165
18	0.1858	18	0.4642	18	0.1476	18	0.3878	L	0.1963	15	0.2606
19	0.0240	19	0.5995	19	0.1879	19	0.4938	M	0.2463	16	0.3127
20	0.3100	20	0.7743	20	0.2392	20	0.6287	N	0.3117	17	0.375
		21	1.000					P	0.3848	18	0.4513
		22	1.2916							19	0.5424
		23	1.6681							20	0.6518
		24	2.1544								

Eddie Smart [16], proposed a throat and nozzle combinations in terms of the parameters b and A_s, that are implementable in practical applications. This represents a set of constraints as explained in Section 4. The feasible relationships between b and A_s are depicted in Table 2.

Table 2. Search region considering practical implementations for Guiberson HJPs.

Geometry	B0	B1	B2	B3	B4	B5	B6	
b	0.9135	0.6643	0.5026	0.3942	0.3025	0.2500	0.2102	
As	0.0009	0.0048	0.0094	0.0146	0.0219	0.0285	0.0357	
Geometry	C1	C2	C3	C4	C5	C6	C7	
b	0.8601	0.6508	0.5104	0.3917	0.3237	0.2721	0.2316	
As	0.0020	0.0066	0.0118	0.0191	0.0257	0.0329	0.0408	
Geometry	D3	D4	D5	D6	D7	D8	D9	
b	0.7344	0.5637	0.4658	0.3916	0.3333	0.2678	0.2201	
As	0.0064	0.0137	0.0203	0.0275	0.0354	0.0484	0.0627	
Geometry	E4	E5	E6	E7	E8	E9	E10	E11
b	0.7675	0.6342	0.5332	0.4539	0.3646	0.2998	0.2505	0.2017
As	0.0073	0.0139	0.0211	0.0290	0.0420	0.0563	0.0721	0.0954

6. Results

In this work the vector design is set as $\mathbf{x} = [x_1, x_2, x_3, x_4]^T = [A_{th}, A_n, P_s, q_1]^T$ and the parameters of the DEA are set to $F = 0.7$ and $CR = 0.8$. The algorithm was implemented in Matlab ©.

It is important to remark that in order to implement the considerations presented in Tables 2 and 1, indexed lists are used in the DEA, i.e. any list item can be identified by a sequential integer number that identifies its position. In order to keep operational conditions feasible, as indicated by the technical data-sheet of the surface pumps, the range of values for the input flow and input pressure were set to minimum and maximum values as: $q_{1_{min}} = 600[BPD]$, $q_{1_{max}} = 1500[BPD]$, $P_{s_{min}} = 900[Psi]$ and $P_{s_{max}} = 2500[Psi]$. Table 3 depicts testing parameters experimentally obtained, [9].

Table 3. Testing coefficients.

σ	1.35 [-]
K_j	0.15 [-]
K_d	0.1 [-]
K_s	0.0 [-]
K_t	0.28 [-]

In order to validate our design proposal, it has been evaluated a set of ten oil-wells from the asset *Aceite Terciario del Golfo* (ATG-Mexico), an important oil-well zone in Mexico. The values of the operating oil-well conditions that have been used to perform this analysis have been provided by the Mexican Company Geolis/Nuvoil (Table 4). In this Table, it can be observed low efficiencies and high power consumption for most oil-wells currently operating. It is important to mention that the efficiency and horsepower consumption, were actually computed with models considered in this paper, based in the operational parameters of the Geolis/Nuvoil Company.

Table 4. Field data of ten wells form ATG-Mexico. (HP= $1.7{\cdot}10^{-5} q_1 \cdot P_s$).

Well	P_f	P_{wf}	q_{max}	h_1	G_w	P_s	q_1	A_n	A_{th}	η [%]	HP
1	3427	2530	373	5248	0.3854	1067	1336	0.0177	0.0452	20.0665	24.2337
2	2700	2182	329	5112	0.3550	995	888	0.0123	0.0380	21.4368	15.0205
3	2700	2182	333	7119	0.3498	1564	974	0.0123	0.0380	18.6433	25.8967
4	2000	1470	129	4917	0.355	924	1141	0.0123	0.0314	4.0318	17.9700
5	1830	1600	250	4331	0.3732	2133	1158	0.0177	0.0452	6.8621	41.9902
6	2567	1539	105	7890	0.3113	1422	868	0.0123	0.0314	7.9871	20.9830
7	1860	1737	250	4934	0.4205	1010	921	0.0123	0.0241	22.8988	15.8136
8	3000	2035	190	4889	0.3585	1209	1425	0.0241	0.0804	7.1149	29.2880
9	2450	2030	300	5243	0.3710	995	772	0.0123	0.0314	22.6438	13.0584
10	3193	3000	260	6562	0.4317	1280	1184	0.0177	0.0804	6.6017	25.7638

6.1 Benchmark oil-well

For the sake of clarity, the sixth oil-well in Table 4 is selected as a benchmark to show our design proposal. Geolis/Nuvoil company disposed of a pressure-temperature sensor of the brand Pioneer Petrotech Services Inc., into the oil-well. The sensor was operating during one month getting the average value of $P_{wf} = 1355[PSI]$, while the predicted with equation (6) is $P_3 = P_{wf} = 1177[Psi]$ getting a error of 13.14 %

After the application of our approach, the first set of results are depicted in Table 6.1, considering the initial population of 20 individuals and varying the number of maximum generations from 50 to 500. As it can be observed with low generations, convergence is not achieved and the optimal efficiency rounds 9% to 11% In these cases the cavitation indicator M is quite lower than M_c and power consumption rounds 40 [HP]. Then, with higher number of generations the efficiency is improved up to 16.88 %, with M closer to M_c. Note also that in this case the power consumption is close to 12 [HP] with a clear energy saving.

Table 5. Numerical results for P=20 and different number of maximum generations.

Generations	A_n	A_{th}	q_1	P_s	HP	P_1	P_2	P_3	η [%]	M	M_c	Time [s]
50	0.0177	0.0241	1436	1511	36.9	3967	2410	398	8.9962	0.0696	0.1071	17.0523
100	0.0123	0.0189	1097	2047	38.2	4503	2560	188	11.4677	0.0940	0.1018	25.7528
150	0.0095	0.0143	706	911	10.9	3367	1948	372	15.7920	0.1422	0.1573	35.1284
200	0.0095	0.0143	704	905	10.8	3361	1948	379	15.8050	0.1424	0.1590	42.2058
250	0.0109	0.0189	839	1029	14.7	3485	1967	275	13.5557	0.1216	0.1923	51.4344
300	0.0075	0.0104	624	2039	21.6	4495	2731	744	16.7122	0.1484	0.1484	64.4303
350	0.0095	0.0143	704	900	10.8	3356	1943	375	15.8147	0.1425	0.1582	29.9908
400	0.0095	0.0104	656	2432	27.1	4888	2944	736	16.0420	0.1413	0.1413	25.9958
450	**0.0075**	**0.0143**	**601**	**1181**	**12.1**	**3637**	**1877**	**152**	**16.8812**	**0.1722**	**0.1722**	**82.6422**
500	0.0095	0.0143	705	905	10.8	3361	1945	374	15.8027	0.1424	0.1580	48.8717

Table 6 presents numerical results by considering a fixed number of $G_{max} = 250$ generations and varying the number of initial population.

As it can be observed, with low initial population and G_{max}

reasonably high, convergence is achieved and the optimal efficiency rounds 15.8% In this cases the cavitation indicator M is quite less than M_c and power consumption rounds 11 [HP], thus saving energy. Nevertheless, in this case with higher number of initial population the efficiency is improved up to 17.23 %, with M equal to M_c and more important, the power consumption is close to 19 [HP]. Here, the geometries selected for A_n and A_{th} are smaller than the selected for the case when the efficiency rounds 16.8 % Moreover, the input pressure must be increased twice in order to render higher efficiency, which explains the 19 [HP] of power consumption.

Table 6. Numerical results for G_{max} =250 and different initial population.

Population	A_n	A_{th}	q_1	P_s	HP	P_1	P_2	P_3	η [%]	M	M_c	Time [s]
50	0.0095	0.0143	704	900	10.8	3356	1944	376	15.8147	0.1425	0.1583	74.04058
100	0.0095	0.0143	704	900	10.8	3356	1943	375	15.8149	0.1425	0.1583	131.5920
150	**0.0075**	**0.0104**	**600**	**1770**	**18.1**	**4226**	**2586**	**750**	**17.2324**	**0.1539**	**0.1539**	181.0629
200	0.0095	0.0143	704	900	10.8	3356	1943	375	15.8149	0.1425	0.1583	243.6755
250	0.0095	0.0143	704	900	10.8	3356	1943	375	15.8149	0.1425	0.1584	177.0426
300	0.0095	0.0143	704	900	10.8	3356	1943	375	15.8149	0.1425	0.1582	258.3238
350	0.0075	0.0104	608	1867	19.3	4323	2641	754	17.0253	0.1517	0.1525	469.1144
400	0.0075	0.0143	600	1178	12.0	3634	1881	163	16.8895	0.1723	0.1780	423.9130
450	0.0095	0.0143	704	900	10.8	3356	1944	376	15.8149	0.1425	0.1584	320.7046
500	0.0075	0.0104	608	1868	19.3	4324	2644	759	17.0113	0.1515	0.1531	474.2681

6.2 Results for the ten wells from ATG-zone Mexico

The rest of the wells were analyzed with the proposed DEA by considering G_{max} = 500 and P = 100. Numerical results are depicted in Table 7. Note that power consumption is between 9 and 19 [HP], remarkably lower than the presented in Table 4. Moreover, the efficiencies are incremented in all cases as shown in Figures 5 and 6. Worst DEA and Best DEA means the worst and best result using the Differential Evolution Algorithm, respectively; while real means the result for the implemented HJP. Note that in most cases $M = M_c$, thus putting in risk of cavitation in the HJP. Nonetheless this result can be improved by considering a safety factor $\beta < 1$ such that $M < \beta M_c$.

Table 7. Results obtained with the DEA algorithm for ten wells form ATG-zone Mexico.

Well	A_n	A_{th}	q_1	P_s	HP	P_1	P_2	P_3	η [%]	M	M_c	Time [s]
1	0.0109	0.0189	600	1015	10.35	3037	2078	1394	34.9052	0.4889	0.4889	203.7145
2	0.0109	0.0189	609	900	9.32	2715	1747	1022	32.7827	0.4375	0.4375	172.1843
3	0.0095	0.0189	662	900	10.14	3390	1839	753	31.0225	0.4434	0.4434	205.3670
4	0.0095	0.0143	605	900	9.26	2646	1561	444	20.1180	0.1953	0.1953	113.0932
5	0.0109	0.0189	654	900	10.01	2516	1450	562	27.4801	0.3298	0.3298	215.3736
6	0.0075	0.0104	608	1868	19.3	4324	2644	759	17.0113	0.1515	0.1531	115.9245
7	0.0095	0.0189	652	900	9.97	2975	1532	422	25.9546	0.3504	0.3504	237.1783
8	0.0095	0.0143	600	1376	14.03	3129	2024	965	25.8551	0.2721	0.2721	177.4631
9	0.0075	0.0143	600	1506	15.36	4338	2361	867	29.0353	0.3842	0.3842	233.4054
10	0.0095	0.0189	607	900	9.29	2845	1542	630	30.9925	0.4426	0.4426	252.6758

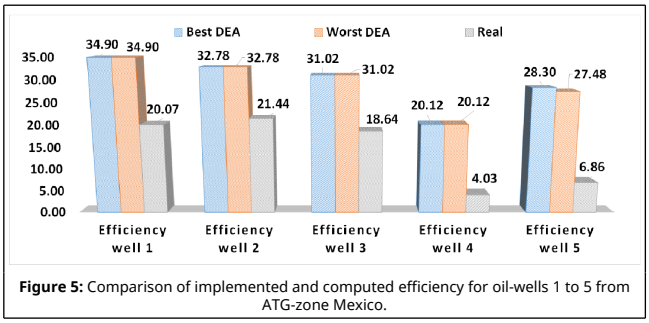

Figure 5: Comparison of implemented and computed efficiency for oil-wells 1 to 5 from ATG-zone Mexico.

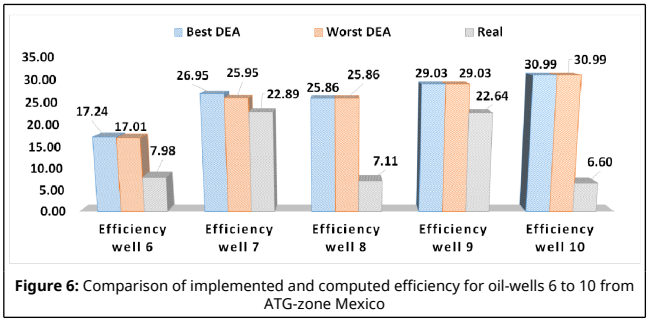

Figure 6: Comparison of implemented and computed efficiency for oil-wells 6 to 10 from ATG-zone Mexico

7. Conclusion

For each oil-well, although belonging to the same productive zone, has different and unique characteristics; for that reason it should always be performed the analysis for each well. The efficiency of an HJP is linked to the implemented geometry. Nevertheless, the analysis must consider the production capacities of each oil-well, as well as the resources available in the installation of the ALS. The algorithm presented in this work is able to define the optimal geometry and the operational conditions that renders the maximum efficiency of the HJP for a given oil-well, based on its characteristics and its production capacities. By using this design methodology it will be easier for the engineers to select the HJP geometries to install besides knowing the efficiency that it can develop during operation while its conditions remain stable.

From the numerical results it can be concluded that efficiency of the operation of the studied wells can be improved up to 24% for a given implementation of the HJP. In addition, it was observed that similar efficiencies can be achieved with different amount of power required to implement the HJP artificial lift system. This fact encourage us to continue research on the optimization of the HJP in terms of the design of other sections such as the inlet holes for the working fluid and suction for the well fluids.

Acknowledgment

The authors would like to thank the support provided by Geolis/Nuvoil for sponsoring, training and advice provided. Their support served extensively for the development and validation of this research article, driving development within the energetic sector in the country.

References

[1] Karassik, I.J., Messina, J.P., Cooper, P. and Heald, C.C.. Pump Handbook. McGraw-Hill. 2001.

[2] Mallela, R. and Chatterjee, D.. Numerical investigation of the effect of geometry on the performance of a jet pump. J. Mech. Eng. Sci. 225:1614 - 1625, 2011.

[3] Mohan, S. and Samad, A.. Jet Pump Design Optimization by Multi-Surrogate Modeling. J. Inst. Eng. India Ser. 96:13-19, 2014.

[4] Saker, A.A. and Hassan, H.Z.. Study of the Different Factors That Influence Jet Pump Performance. Open J. of Fluid Dynamics. 3:44-49, 2013

[5] Xiao, L. and Long, X.. Cavitating flow in annular jet pumps. Int. J. of Multiphase Flow 71:116-132, 2015

[6] Liknes, F.. Jet Pump. Master Thesis. Norwegian University of Science and Technology, 2013.

[7] Fan, J., Eves, J., Thompson, H.M., Toropov, V.V., Kapur, N., Copley, D. and Mincher, A.. Computational fluid dynamic analysis and design optimization of jet pumps. Computers and Fluids. 46:212 - 217. 2011.

[8] White, F. M.. Fluid Mechanics. Mc Graw-Hill. 2004

[9] Brown, K.E..The Technology of Artificial Lift Methods., Vol. 2b. Petroleum Publishing Co. 1993.

[10] Vogel, J. V.. Inflow Performance Relationships for Solution-Gas Drive Wells. J. Pet. Technol. 20:83-92, 1968.

[11] Cunningham, R.G., Hansen, A.G. and Na, T.Y.. Jet Pump Cavitation. ASME. J. Basic Eng. 3 92:483-492, 1970.

[12] Astegui, Y.A.. Modelación y Simulación de un Sistema Centralizado de Bombeo Hidráulico Tipo Jet de un Campo Petrolero, (Master Thesis). Escuela Politécnica Nacional, Facultad de Ingeniería Mecánica, 2011.

[13] Prince, K., Storn, R. and Lampinen, J.. Differential Evolution: a practical approach to global optimization. Springer. 2005.

[14] Mezura-Montes, E. and Coello Coello, C. A. and Tun-Morales, E.. Simple feasibility rules and differential evolution for constrained optimization. _MICAI 2004:Advances in artificial intelligence, 707-716. 2004.

[15] Pantoja-García, J.J., Villarreal-Cervantes, M.G., González-Robles, J.C. and Sepúlveda Cervantes, G.. Síntesis óptima de un mecanismo para la marcha bípeda utilizando evolución diferencial. Revista Internacional de Métodos Numéricos para Cálculo y Diseño en Ingeniería. 33:38-153, 2017.

[16] Smart, E.. Jet Pump Geometry Selection. Southwestern Petroleum Short Course, (April 23-25, 1985, Texas Tech University).